Journal of Pioneering Medical Sciences
Received: February 12, 2026 | Accepted: October 25, 2026 | Published: November 05, 2026
Volume 15, Issue 10, Pages 104-113

DOI https://doi.org/10.47310/jpms2026151010



Apoptosis Induction by Benzhydrol-Acetamide in Acute Myeloid Leukaemia Kasumi-1 Cells

Abdullahi Olawale Ghazal[1], Nozlena Abdul Samad[2*], Mohamad Nurul Azmi[3], Muath Hekmat Helal[4], Nor Adlin Yusoff[5], Melissa Kilus[6] and Hasan Mohammad Abumahmoud[7]

[1,2,5,6]Department of Toxicology, Pusat Kanser Tun Abdullah Ahmad Badawi, Universiti Sains Malaysia, Kepala Batas, 13200, Pulau Pinang, Malaysia
[3,7]School of Chemical Sciences, Universiti Sains Malaysia, 11800 Minden, Penang, Malaysia
[4]Department of Biomedical Sciences; Faculty of Medicine and Health Sciences, An-Najah National University, Nablus, Palestine

*Corresponding author: Dr. Nozlena Abdul Samad (e-mail: nozlena@usm.my).

©2026 the Author(s). This is an open access article distributed under the terms of the Creative Commons Attribution License (http://creativecommons.org/licenses/by/4.0

Abstract The development of effective anticancer agents is challenging due to toxicity, drug resistance and poor physicochemical properties of current compounds. We synthesised a novel benzhydrol derivative, (4-acetamido(phenyl)phenyl) methyl acetate, through a two-step reduction-acylation process from 4-aminobenzophenone. Structural confirmation was validated via NMR spectroscopy. The compound's cytotoxic potential was evaluated against acute myeloid leukaemia (Kasumi-1) and normal haematopoietic stem cell (CD34+) lines using the MTT assay. The compound showed a time- and concentration-dependent decrease in Kasumi-1 cell viability, with an IC_{50} of 21.30±2.47 µg/mL ($p<0.0001$) at 72 h (~74 µM), indicating moderate effectiveness against Kasumi-1 cells. No significant effect was observed on CD34+ cells; a selectivity index greater than 2.56 indicates substantial selectivity of the compound for cancer cells. In silico predictions indicated the compound's potential to interact with key apoptosis-related proteins. Morphological studies indicated apoptosis-related changes in Kasumi-1 cells, corroborating cytotoxic findings, further validated by flow cytometry and protein expression analyses. These findings highlight the pharmacological potential of (4-acetamido(phenyl)phenyl) methyl acetate, suggesting further chemical modifications to improve anticancer activity and pharmacokinetic properties. Additional mechanistic studies and evaluations in various cancer models are necessary to confirm its therapeutic potential.

Key Words Acetoxychavicol Acetate, Acute Myeloid Leukaemia, Apoptosis, Benzhydrol Derivatives, Cytotoxicity, Kasumi-1 and Molecular Docking

INTRODUCTION

Acute Myeloid Leukaemia (AML) is an extremely malignant haematologic cancer with heterogenous abnormal proliferation of immature white blood cell features [1]. It is the most prevalent adult leukaemia subtype (90% of all new cases) and is responsible for 1.9% of all cancer deaths [2,3]. There are no age restrictions on its incidence, meaning it can affect individuals of all ages. Costa *et al.* [4] report that it is the most common malignancy in children younger than 15 years, with ageing being a significant risk factor. Oza *et al.* reported that smoking increases the risk of death twofold in myeloid leukaemia [5]. Smoking is common and widespread in Malaysia, with approximately 21.3% of individuals being smokers, with several socioeconomic factors further increasing the risks [5,6]. Despite remarkable strides in improving the AML survival rate in recent years, especially among children, reaching 65-70%, the 5-year overall survival rate for AML remains less than 50% and the disease continues to be associated with a high mortality rate [3,7]. Moreover, most AML patients frequently experience relapse, occurring in 40-50% of younger patients and the great majority of elderly patients [7]. Kasumi-1 cells are an immortalised leukaemic cell line that has been widely used as a key model for studying the pathophysiologic characteristics of AML [8]. Chemotherapy remains the "first-line" therapy in AML management, often with a combination of cytarabine and daunorubicin [9]. The inactivation of the active metabolite of cytarabine is reportedly a significant driver of chemotherapy failure in AML [9].

Many potential anticancer candidates are unable to break into the pharmaceutical market due to physicochemical limitations that include poor aqueous solubility, isomerisation,

or rapid inactivation, all of which impair their pharmacokinetics, safety and efficacy [10]. For millennia, plants have served as sources of medicinal compounds, with an estimated two-thirds of earth's population depending on plant-derived drugs [11]. Despite the isolation of numerous drugs from natural sources, the search for bioactive compounds of natural or synthetic origin remains a primary challenge in cancer treatment. Structural modification of existing natural anticancer compounds helps improve their efficacy and availability, which is crucial for enhancing treatment options and overcoming resistance in cancer therapies. Despite the increased focus on developing synthetic alternatives, natural sources still account for a staggering 75% of anticancer compounds [12]. Synthetic compounds, whether designed from scratch or modelled on natural leads, offer several advantages as anticancer agents, including structural optimisation, a detailed understanding of the structure-activity relationship, availability and improved selectivity [13,14].

Shieh *et al.* [14] reported the potential of benzhydrol-type derivatives as an alternative for synthesising refined derivatives of natural compounds. They utilised *ortho*-substituted benzophenones, reducing them to benzhydrols. These benzhydrols could then be modified further accordingly. However, this technique remains largely unexplored. Acetoxychavicol Acetate (ACA) is a natural compound obtained from the rhizomes of *Alpinia galanga*, a plant native to Southeast Asia (Figure 1). ACA has been studied against several cancer cell lines, demonstrating considerable cytotoxicity [15]. Misawa *et al.* [16] tested the cytotoxic activity of synthesized ACA benzhydrol derivatives against multiple myeloma cancer cell lines (HL-60 and IM-9) and elucidated their structure-activity relationship. Their results showed that the effective compounds inhibited the growth of the cells by inhibiting the NF-κB pathway with IC_{50} values <5 μM. They also demonstrated that the fusion of the two phenyl rings—to give three closed rings—caused a total loss of NF-κB inhibition and cytotoxic activity, while non-fused derivatives showed significant NF-κB inhibition.

Owing to the limited therapeutic translation of this compound despite its extensively researched potential, coupled with its stereochemical vantage as a scaffold, we use ACA as the model for our synthetic analogue.

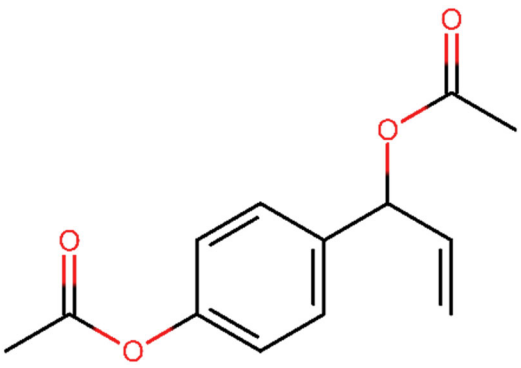


Figure 1: 1'-Acetoxychavicol Acetate

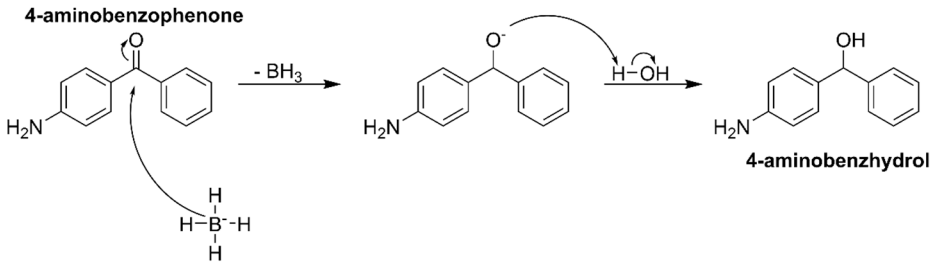
We are not aware of any studies investigating the activity of ACA or its derivatives in Kasumi-1 cells. Furthermore, poor aqueous solubility and stereochemical instability limit its translation into clinical use [17]. Hence, we synthesised (4-acetamido(phenyl)phenyl) methyl acetate as a benzhydrol-type synthetic analogue of ACA and evaluated its inhibitory effects against Kasumi-1 cells. We also employed computational as well as quantitative studies to gain further insights into the mechanics involved in the inhibitory effects being elicited by the test compound.

METHODS

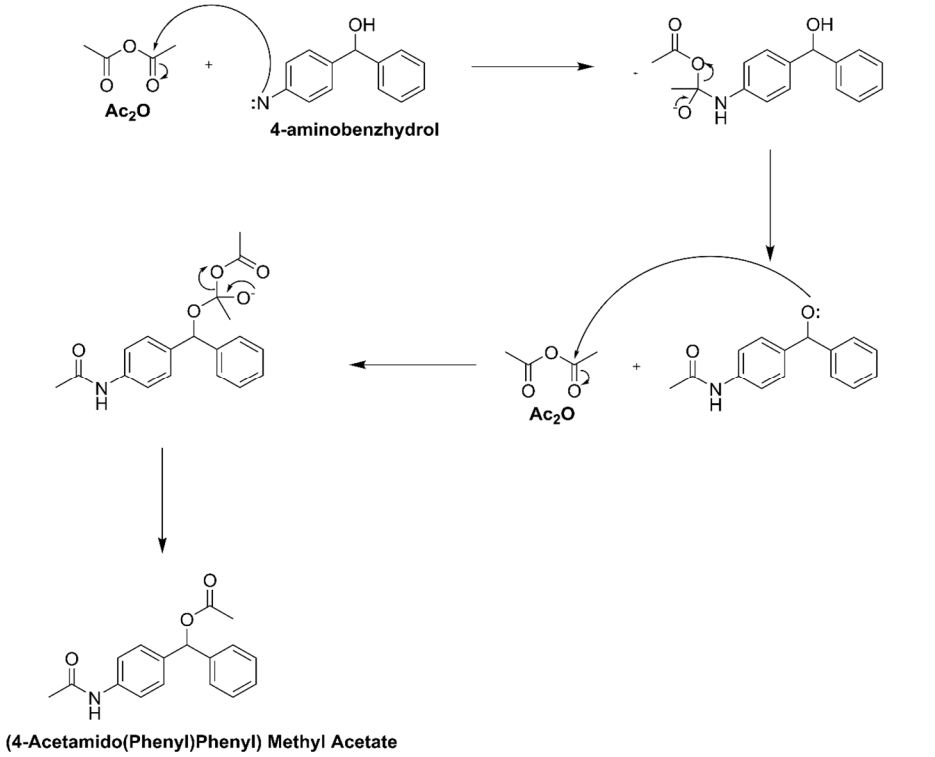
Synthesis of (4-Acetamido(Phenyl)Phenyl) Methyl Acetate (4-AMA)

4-aminobenzhydrol (1, Scheme 1): A 4.11 g of 4-aminobenzophenone (20.86 mmol) was treated with 4 equation of sodium borohydride ($NaBH_4$). This was done in a mixture of tetrahydrofuran (THF) and distilled water (H_2O). The resulting mixture was heated for up to 12 h, resulting in a colourless mixture from the initial pale yellow. A 20 mL of saturated aqueous ammonium chloride was used to quench the mixture before extracting the aqueous layer with 3×20 mL of ethyl acetate (EtOAc). The organic layer was then dried over sodium sulphate (Na_2SO_4), filtered and collected. The resulting compound (4-aminobenzhydrol) was not purified further and was used as is for the next step.

(4-acetamido(phenyl)phenyl) methyl acetate (2, Scheme 2): A 438 mg of the resulting 4-aminobenzhydrol (2 equation) was dissolved in 15 mL of dry dichloromethane and stirred in an ice bath. Subsequently, 536 mg of 2.2 mmol 4-dimethylaminopyridine (DMAP), 620 μL of 2.22 mmol triethylamine (Et_3N) and 0.42 mL of 2.2 mmol acetic anhydride were carefully added with constant stirring. The ice bath was removed after an hour, while the mixture underwent continuous stirring for approximately 12 h. Afterwards, 20 mL of saturated aqueous NH_4Cl was added to quell the reaction. Thin Layer Chromatography (TLC) was employed in monitoring the reaction. The stationary phase comprised *n*-hexane and ethyl acetate in a ratio of 1 to 4. The resulting mixture from the reaction was allowed to stand for 20 min before the aqueous layer was collected using EtOAc, whereas the organic solvents were dried over Na_2SO_4, filtered and collected. The remaining volatile solvents were removed in a rotary evaporator under reduced pressure and the resulting compound was purified via column chromatography, with the separation monitored by TLC. The final compound (4-acetamido(phenyl)phenyl) methyl acetate was obtained as an off-white solid. The chemical structure of the resulting final compound was elucidated via Nuclear Magnetic Resonance (NMR) spectroscopy. ^{1}H NMR (500 MHz, $CDCl_3$, δ/ppm): 2.02 (s, 3H, H-9, $OCOCH_3$), 2.15 (s, 3H, H-11, $NHCOCH_3$), 6.83 (s, 1H, H-7), 7.31-7.49 (m, 5H, H-2′, H-3′, H-4′, H-5′, H-6′), 7.35 (d, J = 8.6 Hz, 2H, H-2, H-6), 7.48 (d, J = 8.6 Hz, 2H, H-3, H-5). ^{13}C NMR (125 MHz, $CDCl_3$, δ/ppm): 21.3 (C-11), 22.7 (C-9), 76.4 (C-7), 119.8 (C-3, C-5), 127.0 (C-2, C-6), 127.9 (C-2′, C-4′, C-6′), 128.5 (C-3′, C-5′), 136.1 (C-1′), 137.6 (C-1), 140.1 (C-4), 168.4 (C-10), 170.1 (C-8).



Scheme 1: Initial Reduction of Starting Compound to Yield Key Intermediary



Scheme 2: Stepwise Formation of (4-acetamido(phenyl)phenyl) Methyl Acetate from Key Intermediary: 4-Aminobenzhydrol

Molecular Docking

Select apoptosis-related proteins were identified and acquired using a search combination of UniProt [18] and RSCB Protein Data Bank [19] databases. PrankWeb [20] was used to determine the chain with the highest binding probability. The criteria for selection were the following: (a) <3 Å resolution, (b) 0% Ramachandran outliers and (c) no mutation. Afterwards, AutoDockTools (v1.5.7) [21] was used to prepare the protein before running the docking using AutoDock Vina (v1.1.2) [22], integrated into PyRx [23]. The proteins were prepared by removing water molecules, as well as any ligands present. The protein was shaved down to the needed chain, processed and readied for docking. The ligand (4-AMA) was run (as 'blind docking') against the protein (chain) with an exhaustiveness of 100. Due to running the docking as 'blind' for each protein, the grid box dimensions are collectively reported in Table S1. Upon completion, the results (2D interactions) were visualised using BIOVIA Discovery Studio Visualizer (v25.1.2484; Dassault Systèmes, France).

Cell Viability Study

Cryopreserved Kasumi-1 cells (ATCC, Manassas, VA) were thawed and cultured in Complete Growth Medium (CGM). The growth medium consisted of RPMI 1640 media (Elabscience Biotechnology Inc., USA), supplemented with 10% v/v foetal bovine serum (TICO EUROPE, Netherlands) and 1% v/v penicillin-streptomycin (Elabscience Biotechnology Inc., USA). The cells were incubated [NB: "incubated" refers to 37°C and 5% CO_2 humidity unless otherwise stated in the text] until 80% confluence. The colorimetric MTT assay was used to evaluate the effects of (4-acetamido(phenyl)phenyl) Methyl Acetate (4-AMA) on the viability of the cells. Kasumi-1 cells were seeded into 96-well microplates at a density of 1×10^4 cells per well. The microplates were then incubated for 3 h prior to treatment with varying concentrations of 4-AMA. Dimethyl Sulfoxide (DMSO) (Sigma-Aldrich Co., USA) was used as a negative control. After incubating for 24, 48, or 72 h, the cells (in the plate) were centrifuged at 1500 rpm for 8 min before

removing the supernatant from each well. Afterwards, 100 µL of 10% v/v MTT solution (in RPMI 1640 medium) was added into each well. The plate was then incubated for 3 h before centrifuging again at 1500 rpm for 8 min. The supernatant was discarded. Subsequently, 30 µL of analytical-grade DMSO (Classic Chemicals, Malaysia) was added into each well. The plate was gently shaken for 5 min on a plate shaker. The Optical Density (OD) of each well was measured at 570 nm and 620 nm using a Multiskan SkyHigh microplate reader (Thermo Fisher Scientific Inc., USA). The IC_{50} of the compound was calculated using the AAT Bioquest Online Calculator. Similarly, the viability of CD34+ (normal haematopoietic stem cells) cells was evaluated following treatment with (4-acetamido(phenyl)phenyl) methyl acetate for 24 h. All experiments were conducted in triplicates, with the mean IC_{50} value reported across all time points and cell types. The cells were grown in three separate culture flasks before starting the procedure, thus ensuring reproducibility of results regardless of growth conditions. Further studies from here on were carried out using the 24 h IC_{50} of 4-AMA. This was done to highlight the notable effect of 'early apoptosis' induced by the compound.

Morphological Study

Kasumi-1 cells were seeded at a density of 1×10^6 in 2.5 mL of CGM. The cells were then incubated for 3 h prior to 4-AMA treatment. The cells were then treated with the 24 h IC_{50} value of the test compound 39 µg/mL. Another group of cells of equal density was treated with a corresponding concentration of DMSO. The final volume was brought up to 5 mL and the cells were incubated for 24 h. As done during the MTT assay, the experiment was conducted in triplicates and the characteristic features were observed across all three sets via microscopic imaging.

Cell Cycle Analysis

The cells were collected, washed and resuspended in 5 mL serum-free media for 24 h to synchronise them to the G_0 phase. The cells were then collected by centrifugation at 1000 rpm for 5 min before seeding 1×10^6 cells per 10 mL of CGM in six separate flasks. Following incubation for three hours, the cells were treated with 4-AMA and DMSO (three flasks per compound) and incubated for 24 h. Subsequently, cells were centrifuged at 1000 rpm for 5 min, washed with 1 mL of PBS (Sigma-Aldrich Co., USA), centrifuged again and resuspended in 400 µL of cold PBS. Cells were fixed in 70% ethanol, added dropwise with constant vortexing and stored at 4°C. Before analysis, the cells were equilibrated to room temperature [23.2-24.1°C depending on the day of the experiment]. The solution was gently inverted and then centrifuged at 1000 rpm for 10 min. The supernatant was discarded and the cells were washed with 1 mL of cold PBS before centrifugation at 1000 rpm for 10 min. A staining solution was prepared with 1 mL PBS, 0.1 µL Triton X-100 (Sigma-Aldrich Co., USA) and 0.5 µL RNase A (Thermo Fisher Scientific Inc., USA) per sample/flask. The pelleted cells were resuspended in the staining solution and incubated at room temperature for 25 min before adding 25 µL of 1 mg/mL Propidium Iodide (PI) and mixing thoroughly. The solution was covered with aluminium foil to shield it from light and incubated at room temperature for 10 min before being placed on ice. The fluorescence of stained cells was measured using a BD FACSCalibur (BD Biosciences, USA) flow cytometry machine and results were analysed with ModFit LT (Verity Software House, USA) software.

Annexin-V/FITC Study

Cells were collected and seeded at a density of 5×10^5 cells per 5 mL of CGM on a 6-well plate. The plate was incubated for 3 h before treating with 4-AMA and DMSO. The plate was incubated for 24 h, after which the cells were centrifuged at 300 xg for 5 min, washed with 1 mL of PBS and centrifuged again. Pelleted cells were prepared using the Annexin V-FITC/PI Apoptosis Kit (Elabscience Biotechnology Inc., USA) following the manufacturer's protocol. The cells were transferred to BD tubes and suspended in 500 µL of 1x Annexin V binding buffer. 5 µL of Annexin V-FITC and PI were added to each tube. The tubes were flicked to mix and then allowed to stand at room temperature for 20 min. The tubes were covered with aluminium foil to block direct light. Subsequently, the tubes were placed in an ice bath before analysis. The fluorescence of the cells was measured using a BD FACSCalibur (BD Biosciences, USA) flow cytometry machine and the results were analysed.

Protein Expression Study

Kasumi-1 cells were seeded at a density of 1×10^6 cells in 10 mL CGM, incubated for 3 h and treated with 4-AMA and DMSO. The cells were then prepared for the assay using both the RayBio® G-Series Human Apoptosis Antibody Array 1 Kit (RayBiotech Inc., USA) and BCA Protein Colorimetric Assay Kit (Elabscience Biotechnology Inc., USA), according to their manufacturer instructions.

Statistical Analysis

Most of the experiments were conducted in triplicates, with the exception of the protein expression study, which used duplicates. Data are presented as the mean ± standard deviation of the three runs and the 95% Confidence Interval (CI) calculated, where possible. Two-way ANOVA was used to determine the significance across time and concentration for Kasumi-1 cells inhibitory study, along with post-hoc comparisons. $P<0.05$ was considered the benchmark for significance, where applicable. All statistical tests were performed using GraphPad Prism (v10.4.1, GraphPad Software, LLC).

RESULTS AND DISCUSSION

Synthesis of (4-Acetamido(Phenyl)Phenyl) Methyl Acetate

(4-acetamido(phenyl)phenyl) methyl acetate (Figure 2) was developed as a benzhydrol-type derivative of acetoxychavicol acetate.

The compound was synthesised in a relatively non-complex process (Scheme 3). The intermediary compound, 4-aminobenzhydrol, was generated following reduction of the ketone to a hydroxyl functional group. By using a weak, selective reducing compound-$NaBH^4$-we were able to attack the oxygen on C2, allowing for its reduction to hydroxyl.

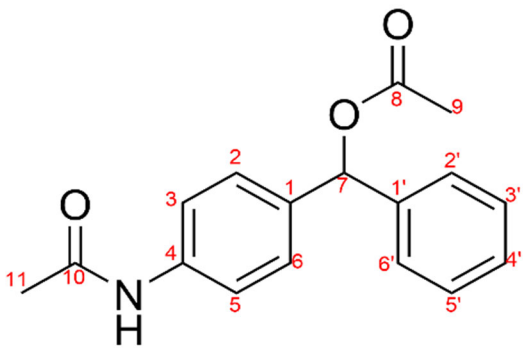
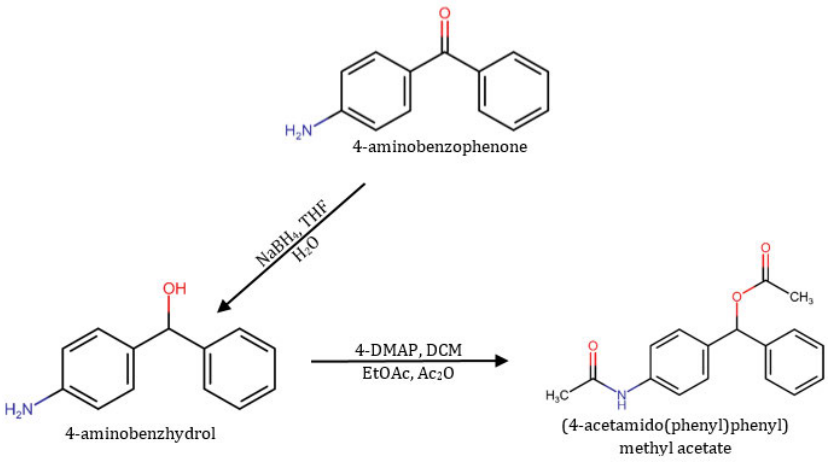


Figure 2: (4-Acetamido(Phenyl)Phenyl) Methyl Acetate



Scheme 3: Illustration of the Synthesis of (4-acetamido(phenyl)phenyl) Methyl Acetate

This step replaced the more electrophilic -C=O with the less electrophilic -OH, enabling the compound to further undergo nucleophilic substitution. 4-aminobenzhydrol was then used to form the final compound, (4-acetamido(phenyl)phenyl) methyl acetate. In this step, the -OH group at C2, as well as the -NH_2 group, was subjected to nucleophilic substitution with 4-DMAP as a catalyst for the acylation reaction. The resulting compound's characterisation via NMR (nuclear magnetic resonance) spectroscopy supports the formation of our compound with substantial accuracy (Figures S1 and S2).

According to the method outlined by Azmi *et al.* [17] in which their starting material was 4-hydroxybenzophenone, we chose 4-aminobenzophenone as our starting material, as its NH_2 functional group is more reactive in nucleophilic reactions than -OH. Further, despite the work of Shieh *et al.* [14] on *ortho*-substituted benzophenones, the stability conferred on both phenyl rings of our compound by the π-system makes the *ortho* position less accessible than other positions given that the carbon connecting both rings is attached at their ipso positions. This makes the compound less flexible, preventing *ortho* substitutions. Thus, we used 4-aminobenzophenone—a *para*-substituted compound—to allow for improved bioactivity owing to better electronic alignment and absence of steric hindrance from the π-system. This is supported by a review on coumarin-chalcone derivatives [24-26] which highlights the improved bioactivity of *para*-substituted derivatives, resulting from improved targeted binding of such compounds. In addition, the polarity of the acetamide moiety may enhance the compound's solubility and further improve activity by allowing hydrogen bonding with protein targets, offering augmented stability and more potential bioactivity than ACA.

Molecular Docking

Upon completing each run of the docking, the highest binding affinity was recorded and the results were saved. The docking was 'blind', as the majority of the proteins had no ligand of similar bioactivity. Table 1 presents the binding affinity of (4-acetamido(phenyl)phenyl) methyl acetate to the selected apoptotic proteins. The receptor-ligand interactions are illustrated in Figure S3a-f. Molecular docking is a mathematical technique aimed at predicting the preferred orientation a molecule employs in a ligand-receptor complex, relative to another molecule, when they are cross-linked to yield a stable complex [19,20].

Binding affinities are often defined using empirical ranges; thus, we define the ranges as weak (≥ −5 kcal/mol), moderate (−5 kcal/mol to −7 kcal/mol), good (≤ −7 kcal/mol) and exceptional (≤ −10 kcal/mol) [27]. (4-acetamido(phenyl)phenyl) methyl acetate showed moderate binding affinity with several docked proteins, with BID showing the highest binding affinity at −7.5 kcal/mol.

Table 1: Binding Affinities of (4-acetamido(phenyl)phenyl) methyl Acetate with Select Proteins

Apoptotic Protein (PDB Code)	Binding Affinity (kcal/mol)	Active Sites	
		Hydrogen Bond	Hydrophobic Bonds
Caspase-3 (1NME)	−5.5	A:ASN141	A:LYS138 A:LYS138
Caspase-8 (1QTN)	−5.9	A:GLU290	A:LYS297 A:GLN339
p53 (2AHI)	−6.2	–	C:PRO98 C:THR256 C:LEU264
p21 (2ZVV)	−6.5	A:TYR133 A:PRO234 A:ALA252	A:ILE128 A:PRO129 A:PRO234 A:TYR250
BID (5AJJ)	−7.5	–	A:ALA130 A:PHE135 A:ILE140
NF-κB (7LEQ)	−6.5	E:HIS418	E:VAL414 E:VAL417 E:ALA451 E:LYS459 E:LEU460 E:MET463

Table 2: Cell Viability of Kasumi-1 and CD34+ Cells Following (4-acetamido(phenyl) phenyl) Methyl Acetate Treatment

Incubation Interval	IC_{50} against Kasumi-1 (µg/mL)	IC_{50} against CD34+ (µg/mL)
24 h	39.27±6.10	>100*
48 h	34.24±3.34	n/a
72 h	21.30±2.47	n/a

*CD34+ cells were only tested at 24 hours post-treatment

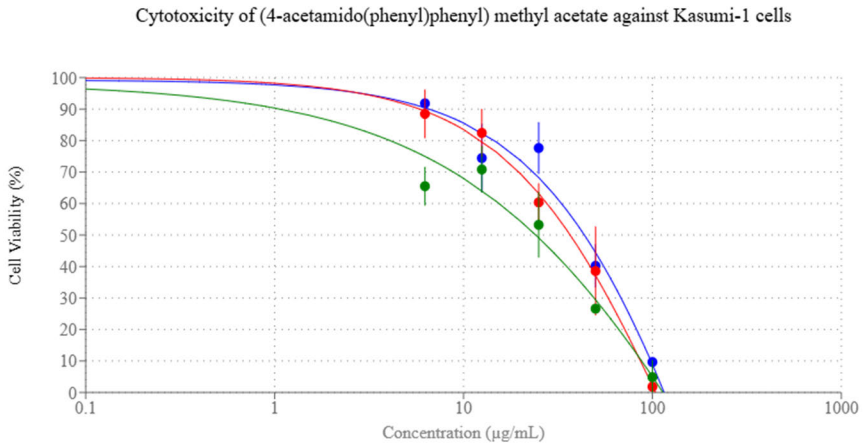


Figure 3: Dose-Response Curve of 4-AMA against Kasumi-1 Cells [blue = 24 h; red = 48 h; green = 72 h]

Both caspase-3 (−5.5 kcal/mol) and caspase-8 (−5.9 kcal/mol) only demonstrated moderate binding affinity. In addition, the majority of the bonds were hydrophobic, which may suggest that the aryl ring(s) are key for bioactivity. Noteworthily, the compound contains relatively short side chains-acetamide and acetoxy groups. Short side chains reportedly exert less influence on its activity [28]. Therefore, replacing these with longer side chains could increasingly influence bioactivity.

Cell Viability Assay

The antiproliferative activity of (4-acetamido(phenyl)phenyl) methyl acetate against Kasumi-1 and CD34+ cells is shown in Table 2 as the half-maximal concentration (IC_{50} values) following treatment.

(4-acetamido(phenyl)phenyl) methyl acetate exhibited a concentration- and time-dependent cytotoxic response against Kasumi-1 cells, evidenced by the graph plot (Figure 3). However, there was no observed activity against CD34+ cells (Figure S4). At 24 h, the IC_{50} of 4-AMA was 39 µg/mL [CI_{95} = 31.24-46.78 µg/mL; p = <0.0001], reducing to 34 µg/mL [CI_{95} = 26.08-38.65 µg/mL; p = <0.0001] after 48 h and 21 µg/mL [CI_{95} = 15.36-27.26 µg/mL; p = <0.0001] after 72 h. This significance evidently supports the dose- and time-dependent inhibitory action of 4-AMA. Post-hoc comparisons also show significance across different concentrations at each timepoint, as most pairs of concentrations (compared) differed by more than 19.16% (Tukey's HSD).

Contrarily, there was no noticeable impediment to viability in CD34+ cells after 24 h exposure to the test compound. The cells remained viable (≥ 90%) at 100 µg/mL the highest concentration tested for Kasumi-1 cells. As there is no definitive IC_{50} value against CD34+ cells, if we take $IC_{50} > 100$ µg/mL, then the Selectivity Index (SI) of 4-AMA will be:

$$SI > \frac{IC_{50}\ (normal\ cells)}{IC_{50}\ (cancer\ cells)} = \frac{100}{39} = 2.56$$

An SI greater than 2.56 (CD34+ Vs Kasumi-1 at 24 h) indicates a modest but statistically significant preference of 4-AMA for leukaemia cells over normal haematopoietic progenitors. According to community-wide accepted standards [29], the anticancer potential of new compounds is defined as 'highly potent' if < 1 µM, 'effective' if between 1 and 10 µM, 'moderate' if between 11 and 99 µM and 'low' if ≥ 100 µM. We calculated the compound's molecular weight [283.3 g/mol] and converted the calculated IC_{50} value to micromolar. At 72 h, the compound's IC_{50} value corresponds to approximately 74 µM, which can be considered moderate. In contrast, at a concentration exceeding 100 µg/mL (≈ 353 µM), the compound is considerably ineffective against CD34+ cells.

Cell Morphology Study

Figures 4 and 5 show the captured distinct microscopic features observed following treatment of Kasumi-1 cells with (4-acetamido(phenyl)phenyl) methyl acetate. Healthy Kasumi-1 cells have a slightly round to oval shape, with smooth contours. This shape is apparent in Figure 4. The cells treated with DMSO showed few signs of injury, with most retaining their original shape.

However, in Figure 5 (4-acetamido(phenyl)phenyl) methyl acetate-treated cells there is evident injury to a substantial number of cells, with the cells displaying morphological features characteristic of apoptosis. These morphological features validate our hypotheses that (4-acetamido(phenyl)phenyl) methyl acetate can induce apoptosis in cancer cells.

Flow Cytometry Studies

In the cell cycle analysis, results from flow cytometry are depicted as clustered columns (Figure 6). The DMSO-treated cells (control group) exhibited a significantly higher percentage in the G_1 phase compared to the cells treated with 4-AMA (treatment group) [64.17% Vs 54.07%; p = 0.00036], which consequently led to the treatment group exhibiting a higher percentage of cells in the S phase compared to the control group [32.53% Vs 24.25%; p = 0.00035]. Significant cell accumulation in the S phase suggests that 4-AMA arrests the cells at this phase of the cycle.

For the Annexin-V/FITC study, the cell progression to programmed death (apoptosis) is illustrated as clustered columns, with each column representing a quadrant population (Figure 7). Similarly, these populations represent pathophysiologic outcomes following exposure to a pharmacological agent: necrotic cells (PI+/Annexin− stained), late-stage apoptosis (PI+/Annexin+ stained), viable cells (PI−/Annexin− stained) and early apoptotic cells (PI−/Annexin+ stained).

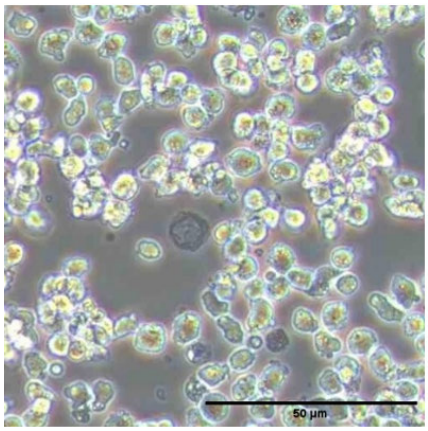


Figure 4: DMSO-Treated Cells at 200x Magnification after 24 h

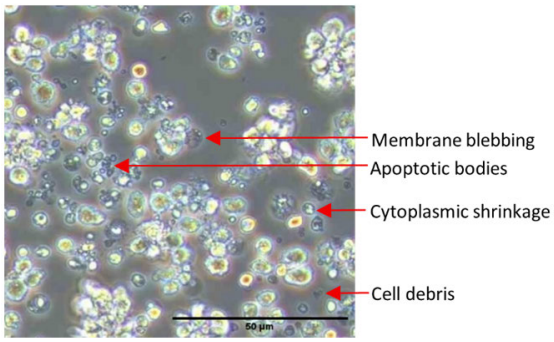


Figure 5: 4-AMA-Treated Cells at 200x Magnification after 24 h

4-AMA significantly induced early apoptosis in the cells compared to DMSO [8.81% Vs 5.29%; p = 0.043]. No statistical difference was found between the groups for healthy cells (p = 0.188), late apoptotic cells (p = 0.396) and necrotic cells (p = 0.543). Increased early and late apoptotic cells suggest potential DNA fragmentation in cells treated with 4-AMA. In addition, the progression to necrosis was minimal—an equally desirable outcome.

Protein Expression Study

The kit used allowed for the targeting of up to 43 different apoptosis-related proteins; however, only those of significance are shown here. Figure 8 displays the results in clustered columns as the fold change in protein expression between DMSO-treated and 4-AMA-treated cells (that is, the expression in treatment cells divided by the expression in control cells). Table S2 gives a full list of the expression signals of all 43 proteins across both treatment groups. Proteins that had decreased expressions in 4-AMA compared to DMSO are presented as inverted columns. A fold increase of ≥1.5 or decrease of ≤0.5 was considered significant and the columns are coloured green or red, respectively.

Four apoptosis-related proteins were significantly overexpressed, while two were notably underexpressed. BID, Caspase-3, HSP27 and sTNF-R2 were overexpressed above the cutoff, with caspase-3 showing the most significant increase.

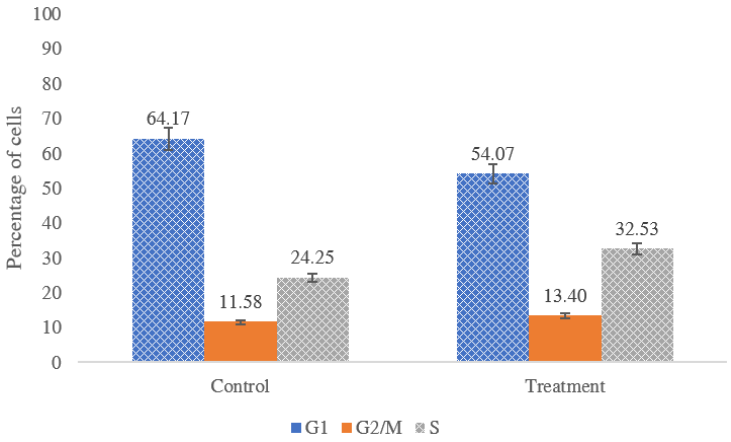


Figure 6: Columnar Distribution of Kasumi-1 Cells 24 h Following Treatment with 4-AMA. [*Diamond grid implies "significance"*]

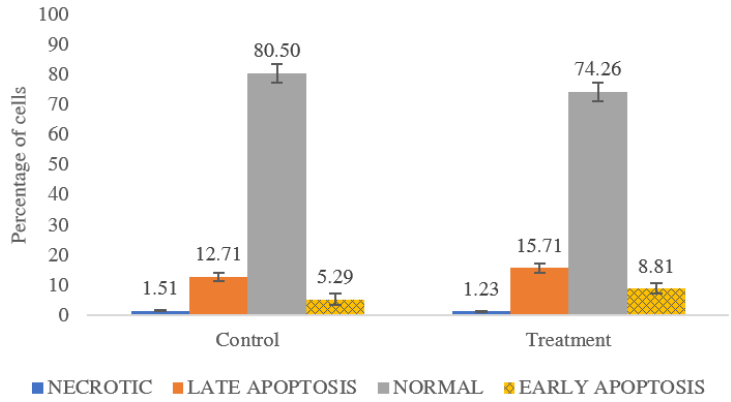


Figure 7: Graphical Representation of the Four Population Groups after 24 h of Treatment. [*Diamond grid implies "significance"*]

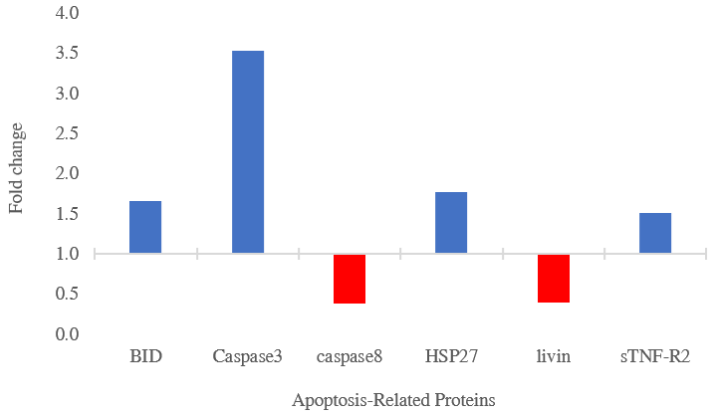


Figure 8: Change in Expression Levels of Select Proteins 24 h after Treatment with 4-AMA

In the molecular docking study, the binding affinity of 4-AMA to caspase-3 was the lowest of all docked proteins at −5.5 kcal/mol. Yet, it exhibited the highest increase in expression following treatment with the test compound. Caspase-3, as an executioner caspase, shows a significant increase in expression. Aggregating this two contrasts, it may be that the increased expression of caspase-3 presents more as a cumulative effect of several pro-apoptotic proteins (including those slightly below the cutoff), rather than solely as a direct one. BID is a pro-apoptotic member of the Bcl-2 family that plays a role in the intrinsic apoptosis pathway [30]. The significant increase in expression enhances the apoptosis-inducing ability of 4-AMA.

sTNF-R2 is the soluble form of TNF-R2, an anti-apoptotic protein that recruits c-IAP1 and c-IAP2 [31]. Increased expression of several IAPs (inhibitors of apoptosis proteins) is associated with resistance in various cancer types, disease progression and poor prognosis [32,33].

There was no significant difference in c-IAP2 expression after treatment with the test compound. The second most notable increase in expression, after caspase-3, was seen in HSP27. This protein protects cells and promotes survival under stress conditions [34]. Increased expression indicates cellular injury and stress, leading to elevated HSP27 levels that counteract apoptosis and enhance survival in Kasumi-1 cells. In the annexin V assay, cell progression into early and late apoptosis was hindered. Results from the targeting assay confirm this impedance, as the anti-apoptotic proteins (sTNF-R2 and HSP27) simultaneously counteract the cytotoxic effects of 4-AMA induced via interactions with the pro-apoptotic proteins, caspase-3 and BID.

Conversely, two proteins exhibited significantly reduced expression after 4-AMA treatment. Caspase-8 is an essential initiator caspase in the extrinsic apoptosis pathway [35]. The downregulation of caspase-8, a key initiator caspase, highlights the complexities of the pharmacodynamics related to the test compound's action. Kasumi-1 cells undergo apoptosis with minimal involvement of caspase-8 [33-36]; highlighting the intrinsic pathway's primary role in these cells, as supported by our findings. Huang et al. noted that apoptosis in Kasumi-1 cells may inversely correlate with survivin expression levels [37]. Thus, the caspase-8 paradox supports a potential resistance mechanism in Kasumi-1 cells by significantly increasing IAP expression, leading to reduced caspase-8 levels.

CONCLUSION

(4-Acetamido(phenyl)phenyl) methyl acetate was synthesised and characterised, exhibiting moderate, time-dependent selective cytotoxicity against Kasumi-1 acute myeloid leukemic cells. Despite its moderate cytotoxic potency, 4-AMA exhibited morphological and biochemical characteristics indicative of apoptosis, highlighting its therapeutic potential. Molecular target prediction and mechanistic investigations offered insights into the pathways underlying its biological activity. 4-AMA, a benzhydrol-type analogue of ACA, demonstrates that structural modifications of lead compounds can affect biological activity and pharmacological properties. The stereochemical features of 4-AMA may enhance its favourable characteristics and require further investigation. This study enhances the understanding of ACA-derived compounds by showing the inhibitory effects of 4-AMA on Kasumi-1 cells and its potential as a scaffold for future optimisations. This work establishes a basis for the further development and optimisation of ACA-derived compounds as potential anticancer agents for acute myeloid leukaemia. This study had some limitations. First, we used only NMR in characterising the final compound. Hence, the results should be validated using other characterisation techniques. Second, the molecular docking was done 'blindly' owing to a lack of similar ligands in the tested proteins; thus, the results should be interpreted with caution. Third, only one AML cell line Kasumi-1 was used in the evaluation of this compound. This should not preclude the therapeutic capability of 4-AMA and the compound should be tested on other AML and non-AML cell lines. Additionally, the study should be further validated via in vivo studies.

Acknowledgement

The authors are grateful to their departments and Universiti Sains Malaysia.

Funding

This work was supported by a Universiti Sains Malaysia Bridging Grant with Project No: R501-LR-RND003-0000002094-0000.

Data Availability

All data supporting the findings of this study are available within the paper and its supplementary information.

Author Contributions

AOG: Investigation, Formal analysis, Data curation, Visualisation, Writing-Original Draft, Writing-Review and Editing. NAS: Conceptualisation, Methodology, Validation, Resources, Supervision, Funding Acquisition. MNA: Resources, Supervision. MHH: Supervision, Writing-Review and Editing, Validation. NAY: Molecular Docking, Supervision. MK: Writing-Review and Editing. HMA: Synthesis and Characterisation.

Competing Interests

The authors have no competing interests to declare that are relevant to the content of this article.

REFERENCES

[1] Pardhi, E. *et al.* "Multifunctional targetable liposomal drug delivery system in the management of leukemia: Potential, opportunities and emerging strategies." *Life Sciences*, vol. 325, 2023, article 121771. DOI: 10.1016/j.lfs.2023.121771.

[2] Algariri, E.S. *et al.* "The characterization of acute myeloblastic leukemia-M2 cell lines with Suppressed Stromal Interaction Molecule 1 (STIM1) and its impact on calcium/reactive oxygen species profiles." *Journal of Angiotherapy*, vol. 8, 2024. DOI: 10.25163/angiotherapy.819435.

[3] Kawakatsu, R. *et al.* "The combination of venetoclax and quercetin exerts a cytotoxic effect on acute myeloid leukemia." *Scientific Reports*, vol. 14, 2024, article 26418. DOI: 10.1038/s41598-024-78221-9.

[4] Costa, R.G.A. *et al.* "Emerging drugs targeting cellular redox homeostasis to eliminate acute myeloid leukemia stem cells." *Redox Biology*, vol. 62, 2023, article 102692. DOI: 10.1016/j.redox.2023.102692.

[5] Mohd Yusoff, M.F. *et al.* "The pattern in prevalence and sociodemographic factors of smoking in Malaysia, 2011-2019: findings from national surveys." *Tobacco Induced Diseases*, vol. 20, 2022, pp. 1-11. DOI: 10.18332/tid/152410.

[6] Sasaki, K. *et al.* "De novo acute myeloid leukemia: A population-based study of outcome in the United States based on the Surveillance, Epidemiology and End Results (SEER) database, 1980 to 2017." *Cancer*, vol. 127, 2021, pp. 2049-2061. DOI: 10.1002/cncr.33458.

[7] Thol, F. and A. Ganser. "Treatment of relapsed acute myeloid leukemia." *Current Treatment Options in Oncology*, vol. 21, 2020, article 66. DOI: 10.1007/s11864-020-00765-5.

[8] Asou, H. *et al.* "Establishment of a human acute myeloid leukemia cell line (Kasumi-1) with 8;21 chromosome translocation." *Blood*, vol. 77, 1991, pp. 2031-2036. DOI: 10.1182/blood.V77.9.2031.2031.

[9] Schneider, C. *et al.* "SAMHD1 is a biomarker for cytarabine response and a therapeutic target in acute myeloid leukemia." *Nature Medicine*, vol. 23, 2017, pp. 250-255. DOI: 10.1038/nm.4255.

[10] Andreani, T. *et al.* "Natural compounds-based nanomedicines for cancer treatment: Future directions and challenges." *Drug Delivery and Translational Research*, vol. 14, 2024, pp. 2845-2916. DOI: 10.1007/s13346-024-01649-z.

[11] Guillén-Meléndez, G.A. *et al.* "Nanoencapsulation of extracts and isolated compounds of plant origin and their cytotoxic effects on breast and cervical cancer treatments: Advantages and new challenges." *Toxicon*, vol. 244, 2024, article 107753. DOI: 10.1016/j.toxicon.2024.107753

[12] Sharifi-Rad, J. *et al.* "Natural products and synthetic analogs as a source of antitumor drugs." *Biomolecules*, vol. 9, 2019, article 679. DOI: 10.3390/biom9110679

[13] Kojima-Yuasa, A. and I. Matsui-Yuasa. "Pharmacological effects of 1′-acetoxychavicol acetate, a major constituent in the rhizomes of *Alpinia galanga* and *Alpinia conchigera*." *Journal of Medicinal Food*, vol. 23, 2020, pp. 465-475. DOI: 10.1089/jmf.2019.4490

[14] Shieh, W.C. *et al.* "Asymmetric reduction of ortho-substituted benzophenones with B-chlorodiisopinocampheylborane: A convenient synthesis of enantiomerically enriched benzhydrols." *Tetrahedron Letters*, vol. 36, 1995, pp. 3797-3800. DOI: 10.1016/0040-4039(95)00609-G

[15] Baradwaj, R.G. *et al.* "Novel purification of 1′S-1′-acetoxychavicol acetate from *Alpinia galanga* and its cytotoxic plus antiproliferative activity in colorectal adenocarcinoma cell line SW480." *Biomedicine and Pharmacotherapy*, vol. 91, 2017, pp. 485-493. DOI: 10.1016/j.biopha.2017.04.114

[16] Misawa, T. *et al.* "Structure-activity relationships of benzhydrol derivatives based on 1′-Acetoxychavicol Acetate (ACA) and their inhibitory activities on multiple myeloma cell growth via inactivation of the NF-κB pathway." *Bioorganic and Medicinal Chemistry*, vol. 23, 2015, pp. 2241-2246. DOI: 10.1016/j.bmc.2015.02.039

[17] Azmi, M.N. *et al.* "Synthesis of benzhydrol analogues based on 1′-Acetoxychavicol Acetate (ACA), as a stable and potent antiproliferative agent on breast cancer cell lines, ADMET analysis and molecular docking study." *Organic Communications*, 2024, pp. 99-114. DOI: 10.25135/acg.oc.2405.3237

[18] Bateman, A. *et al.* "UniProt: the Universal Protein Knowledgebase in 2025." *Nucleic Acids Research*, vol. 53, 2025, pp. D609-D617. DOI: 10.1093/nar/gkae1010

[19] Burley, S.K. *et al.* "Updated resources for exploring experimentally-determined PDB structures and Computed Structure Models at the RCSB Protein Data Bank." *Nucleic Acids Research*, vol. 53, 2025, pp. D564-D574. DOI: 10.1093/nar/gkae1091

[20] PrankWeb. "PrankWeb: ligand binding site prediction." *PrankWeb*, https://prankweb.cz/. Accessed 11 Sept. 2025.

[21] Sanner, M. F. "Python: A programming language for software integration and development." *Journal of Molecular Graphics and Modelling*, vol. 17, 1999, pp. 57-61.

[22] Trott, O. and A.J. Olson. "AutoDock Vina: Improving the speed and accuracy of docking with a new scoring function, efficient optimization and multithreading." *Journal of Computational Chemistry*, vol. 31, 2010, pp. 455-461. DOI: 10.1002/jcc.21334.

[23] Dallakyan, *et al.* "Small-Molecule Library Screening by Docking with PyRx." Methods in Molecular Biology, 2015, pp. 243-250. DOI: 10.1007/978-1-4939-2269-7_19.

[24] Konidala, S.K. and V. Kotra. "Recent strategies for efficient synthesis and biological activities of coumarin-chalcone derivatives." *Asian Journal of Pharmaceutical and Clinical Research*, vol. 13, no. 5, 2020, pp. 28-37. DOI: 10.22159/ajpcr.2020.v13i5.37039.

[25] Raval, K. and T. Ganatra. "Basics, types and applications of molecular docking: A review." *IP International Journal of Comprehensive and Advanced Pharmacology*, vol. 7, 2022, pp. 12-16. DOI: 10.18231/j.ijcaap.2022.003.

[26] Agu, P.C. *et al.* "Molecular docking as a tool for the discovery of molecular targets of nutraceuticals in diseases management." Scientific Reports, vol. 13, 2023, article 13398. DOI: 10.1038/s41598-023-40160-2.

[27] Yunta, M. "Docking and ligand binding affinity: uses and pitfalls." *American Journal of Modeling and Optimization*, vol. 4, 2016, pp. 74-114. DOI: 10.12691/ajmo-4-3-2.

[28] Essa, A.F. *et al.* "Natural acylated flavonoids: Their chemistry and biological merits in context to molecular docking studies." Phytochemistry Reviews, vol. 22, 2023, pp. 1469-1508. DOI: 10.1007/s11101-022-09840-1.

[29] Şeker Karatoprak, G. *et al.* "A comprehensive review on the potential of coumarin and related derivatives as multi-target therapeutic agents in the management of gynecological cancers." Frontiers in Pharmacology, vol. 15, 2024. DOI: 10.3389/fphar.2024.1423480.

[30] Czabotar, P.E. *et al.* "Control of apoptosis by the BCL-2 protein family: Implications for physiology and therapy." *Nature Reviews Molecular Cell Biology*, vol. 15, 2014, pp. 49-63. DOI: 10.1038/nrm3722.

[31] Siegmund, D. *et al.* "TNF Receptor Associated Factor 2 (TRAF2) signaling in cancer." *Cancers*, vol. 14, 2022, article 4055. DOI: 10.3390/cancers14164055.

[32] Garg, H. *et al.* "Survivin: A unique target for tumor therapy." *Cancer Cell International*, vol. 16, 2016, article 49. DOI: 10.1186/s12935-016-0326-1.

[33] Krawiec, K. *et al.* "Targeting apoptosis in AML: Where do we stand?" *Cancers*, vol. 14, 2022, article 4995. DOI: 10.3390/cancers14204995.

[34] Qi, Z. *et al.* "Phosphorylation of heat shock protein 27 antagonizes TNF-α-Induced HeLa cell apoptosis via regulating TAK1 ubiquitination and activation of p38 and ERK signaling." Cellular Signalling, vol. 26, 2014, pp. 1616-1625. DOI: 10.1016/j.cellsig.2014.03.015.

[35] Green, D.R. "The death receptor pathway of apoptosis." Cold *Spring Harbor Perspectives in Biology*, vol. 14, 2022, article a041053. DOI: 10.1101/cshperspect.a041053.

[36] Rovida, E. *et al.* "The c-Jun-N-terminal-kinase inhibitor SP600125 enhances the butyrate derivative D1-induced apoptosis via caspase 8 activation in Kasumi 1 t(8;21) Acute Myeloid Leukaemia Cells." *British Journal of Haematology,* vol. 135, 2006, pp. 653-659. DOI: 10.1111/j.1365-2141.2006.06365.x.

[37] Huang, J. *et al.* "Influence of survivin-targeted therapy on chemosensitivity in the treatment of acute myeloid Leukemia." *Cancer Letters*, vol. 366, 2015, pp. 160-172. DOI: 10.1016/j.canlet.2015.05.033